Computers & Geosciences 106 (2017) 68–76

Contents lists available at ScienceDirect

Computers & Geosciences

journal homepage: www.elsevier.com/locate/cageo

Research paper

Subsetting hyperspectral core imaging data using a graphic-identification-based IDL program

Jun-Ting Qiu[a,b], Chuan Zhang[a,b,*], Zhang-Fa Yu[a], Qing-Jun Xu[b], Ding Wu[a], Wei-Wei Li[a], Jia-Lei Yao[b]

[a] National Key Laboratory of Science and Technology on Remote Sensing Information and Image Analysis, Beijing Research Institute of Uranium Geology, Beijing 100029, China
[b] School of Earth Sciences and Resources, China University of Geosciences, Beijing 100083, China

ARTICLE INFO

Keywords:
Hyperspectral imaging
HySpex
Drill core
IDL
Subset image

ABSTRACT

This study presents an IDL program to subset hyperspectral drill core imagery automatically based on graphic identification. A HySpex SWIR-320m-e imager and drill cores from the Xiangshan uranium deposit were used to do an application test. Based on the HySpex images, we found that the ratio variation tolerance of 75%, minimum marker size of 37 pixel × 37 pixel (28 mm × 28 mm), and wavelength of 1141.3 nm (band #30) are preferences for the IDL program. The results indicate that the IDL program subsets hyperspectral images with high accuracy and efficiency without consuming additional time during the scanning process. Additionally, deformation of the core box, the material from which the core box is made, and variation in the diameter of the drill core do not significantly affect the quality of the results.

1. Introduction

Hyperspectral imaging, or imaging spectroscopy, enables the digital imaging of geological materials and the measurement of their reflectance spectra in the visible through infrared portions of the electromagnetic spectrum. As every pixel in the image contains a continuous spectrum (in radiance or reflectance), the technique has broad geological uses, such as the identification and characterization of complex mineralogical alteration assemblages (Kruse, 1996; Kruse et al., 2012; Murphy and Monteiro et al., 2013; Tappert et al., 2015; Mathieu et al., 2017), and the correlation of geological units (Baissa et al., 2011; Dorador and Rodriguez-Tovar, 2016). The imagery also includes information about the context and textures of a rock unit, which can help identify faults and fractures, and evaluate the degree of veining or dissemination (Qu et al., 2016). The hyperspectral imaging of drill core provides geologists with a comprehensive and reusable digital data-set for understanding the subsurface geology of a particular area, and so aids their geological surveying and mining work (Kruse, 1996; Kruse et al., 2012; Murphy and Monteiro et al., 2013; Tappert et al., 2015; Speta et al., 2015; Speta et al., 2016; Mathieu et al., 2017).

Given the usefulness of drill core hyperspectral imagery to geologists, many web-based databases and platforms have been established for their storage and sharing,[1,2,3]. Each image usually shows several cores as well as the box that holds the cores. The image contains hundreds of bands and millions of pixels, meaning that it is spectrally and spatially large, which results that it is a big file and slow to download. An effective way to save time and reduce the required storage is to remove redundant pixels by making subsets of the cores from the whole image before uploading the image into the database.

The traditional method of manually assigning creating core image subsets is often problematic and inefficient. For example, using a rectangle subset is inaccurate when the core box is deformed, and the ROI (region of interest) method is laborious, as the operator has to manually draw ROIs before subsetting the image. Some software packages (e.g., ENVI) can create masks based on the differences between the spectral characteristics of the drill core and that of the core box to automatically remove the redundant pixels. Although this is much more convenient than manual work, it is less accurate because the spectrum of the core box can vary, as the box may contain dirt or may be made of a range of materials. A commercial scanning and processing system employing HyLogger and The Spectral Geologist can perform image subsetting automatically, but requires input of the

* Corresponding author at: National Key Laboratory of Science and Technology on Remote Sensing Information and Image Analysis, Beijing Research Institute of Uranium Geology, Beijing 100029, China.
E-mail addresses: midimyself@126.com (J.-T. Qiu), chuanzi521@163.com (C. Zhang).
[1] http://www.corescan.com.au/services/storage-and-visualisation
[2] http://terracoregeo.com/software
[3] http://zkinfo.cgsi.cn

http://dx.doi.org/10.1016/j.cageo.2017.05.009
Received 9 November 2016; Received in revised form 17 May 2017; Accepted 17 May 2017
Available online 24 May 2017

measurements of the core box and the specific arrangement of drill cores in the box. This is also time consuming, especially when the size of the core box and the arrangement of the drill cores vary, as users must measure the core box and then edit the profile file iteratively. Another commercial hyperspectral scanning system, Corescan's HCl3,[4] which is equipped with a laser profilometer, can be used for rapid core masking. However, not all scanning systems contain laser profilometer module, and the hardware upgrade is expensive.

Since, most researchers don't have access to commercial systems, this study presents a free IDL program that automatically subsets hyperspectral drill core images based on graphic identification. Core image data from a HySpex SWIR-320m-e imager was used to evaluate the capabilities and efficiency of the program.

2. Instrument and samples

We used a HySpex SWIR-320m-e hyperspectral imager (Norsk Elektro Optikk AS, NEO) that operates across the short wave infrared (SWIR) portion of the electromagnetic spectrum from 1000 nm to 2500 nm with a spectral sampling interval of 6.25 nm (256 bands). This wavelength range covers the spectral absorptions of hydrous silicates, carbonates, phosphates, sulfates, as well as some hydrothermal alteration minerals, such as calcite, dolomite, chlorite, and sericite. The instrument also produces mineral and textural maps, with a spatial resolution of ~0.75 mm/pixel. The high spectral resolution and sub-millimeter spatial resolution provides distinct advantages in the processing, analysis, and interpretation of spectral characteristics and trends in both alteration assemblages and individual minerals. The technical specifications of the HySpex SWIR-320m-e imager are listed in Table 1.

Spectral data was collected for drill core samples from the Xiangshan volcanic-related uranium deposit. The core samples were ~5.5 and ~3.5 cm in diameter, with variable colors. The lithology of the core samples was dominated by volcanic-related rocks, such as rhyolitic crystal tuffs, welded tuffs, rhyodacites, and acidic porphyritic lava, along with some Mesozoic sedimentary rocks such as red sandstone and mudstone. Alteration minerals in the cores include sericite, chlorite, and carbonate. Some samples also contain hematite bands. The cores are stored in wooden boxes (~100 cm long and 30–50 cm wide). Most of them are covered by dust, paint, mould, iron or plastic clips, thus have variable colors. Some boxes are skew.

3. Methodology and algorithm

3.1. Methodology

This study proposes a graphic-identification-based method to subset the hyperspectral drill core imagery. The method involves two key steps:

1) Four graphic markers are placed along the edges of the core box, to form the fixed vertices of the quadrangle region outlining the subset image.
2) After scanning the drill cores (in their boxes) using the hyperspectral imager, the graphic markers are located in the spectral imagery of cores, the subset regions are created, and the image is subsetted using an IDL program.

Each marker defining a subset region consists of a solid black square surrounded by a white border and a black square outline on a white background; the same pattern is commonly used to mark the corner markers of Quick Response Codes (QR Codes, Fig. 1a). The ratios of the widths of the black outline, the white border, the central solid black square, the white border (again), and the black outline (again) are 1:1:3:1:1 (Fig. 1b, ISO/IEC 18004). The distinctive shape makes the graphic marker easily detectable by a programmed processor using a two-dimensional digital scanning system. Because of its symmetry, the marker center can be detected at any angle (Fig. 1c).

After the markers in the hyperspectral image are identified, the IDL program automatically creates a quadrangle based on the locations (margins are used for more accurate subsetting; Fig. 2a). The program subsets the image according to the outline of the quadrangle, and sets the spectra of pixels outside the quadrangle to zero (Fig. 2b). Fig. 3 depicts the whole process.

Table 1
Technical specification of HySpex SWIR-320m-e imager.

Camera	SWIR-320m-e
Detector	HgCdTe (320 × 256)
Spectral range	1.0–2.5 μm
Spatial pixels	320
FOV across track	14°
Pixel FOV across/-along track	0.75 mrad/ 0.75 mrad
Spectral sample	6.25 nm
number of bands	256
Digitization	14 bit
Max frame rate	100 fps
dimension(lwh in cm)	36 ×14 ×15.2
Sensor head wgt	7.5 kg

Note: the data was sourced from http://www.hyspex.no/products/disc/swir-320m-e.php.

3.2. Processing and algorithm

The entire image processing procedure is shown in Fig. 4 and is described as follows.

3.2.1. Image loading

Band-sequential (BSQ), band-interleaved-by-line (BIL), and band-interleaved-by-pixel (BIP) are three common formats of organizing image data for hyperspectral images. The BSQ format, which is optimal for accessing the image spatial information, improves data processing efficiency for finding graphic markers in the image. Therefore, the program loads the hyperspectral image and converts the file from BIL or BIP format to BSQ format, if necessary.

3.2.2. Band selection

One band of the BSQ file is selected for graphic marker identification. The IDL program must perform image binarization to separate the black and white blocks of the graphic markers before it can identify the marker. It uses the average gray level of the band image as the threshold for binarization. Out of the hundreds of bands, the one with the highest contrast between the black and white blocks is chosen, because a larger contrast maximizes the difference between the image's average gray level and the difference between the reflectance of the black blocks and that of the white blocks.

The contrast between the two blocks in different bands depends on the material of the marker. We printed markers on white A4 paper with a laser printer, which was inexpensive and easy to prepare (other materials can be used but will not be discussed in this study).

Using white A4 paper, the greatest difference in reflectance between the black and white blocks was 0.732, which occurred at 1141.3 nm (band 30; Fig. 5).

3.2.3. Median filtering

To reduce noise, the selected band image was filtered with 3 × 3 median filtering.

[4] http://www.corescan.com.au/

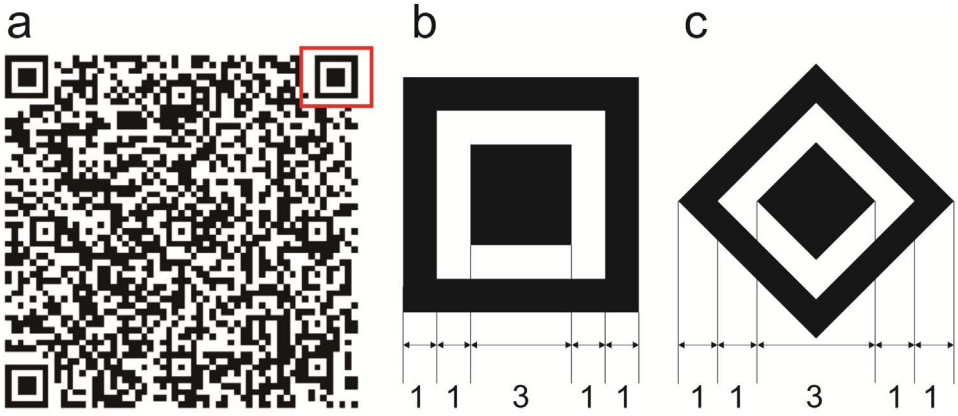

Fig. 1. The graphic marker used as an identifier in this study. (a) The marker is the same as the corner of Quick Response Codes. (b) The ratios of the widths of the black and white blocks of the marker are 1:1:3:1:1. (c) The symmetry of the marker enables it to be recognized at any scanning angle.

Fig. 2. (a) White lines indicate the margins, and red boxes show the quadrangles created by the IDL program. (b) The original image has been subsetted into several images according to the quadrangles created by the IDL program, with pixels outside the quadrangles reset to zero.

3.2.4. Binarization

The filtered image is binarized (Eq. (1)), using the average gray level as the threshold. A monochrome (i.e., 0–1) image is then generated (Fig. 6a, b).

$$\text{Pixel value} = \begin{cases} 1, \ \& \ \text{Pixel value} \geq \text{Threshold} \\ 0, \ \& \ \text{Pixel value} < \text{Threshold} \end{cases} \quad (1)$$

3.2.5. Marker identification

The marker is identified based on its distinctive shape, namely the ratios of the widths among of the black and white blocks (1:1:3:1:1). This pattern is rare in nature; therefore, other shapes and textures in the image will not significantly affect marker identification.

The program first scans along the Y-axis, to search for possible marker center points. It will count the numbers of continuous 0 or 1 in a row of the binary image, and store the numbers in a temporary array, referred to as A (Fig. 6c). If the number of elements (n) in A[n] is fewer than five, the program will count the numbers in the next row or column, while performing a loop from i = 1 to i = n−4 (Fig. 6d). It determines whether r1, r2, r3, and r4 are equal to 1, 1/3, 1, and 1 respectively (Fig. 6e), where r1, r2, r3, r4 are ratios that can be calculated as follows (Eq. (2)–Eq. (5)):

$$\text{r1} = \frac{\text{A[i]}}{\text{A[i + 1]}}, \quad (2)$$

$$r2 = \frac{\text{A[i]}}{\text{A[i + 2]}}, \quad (3)$$

$$\text{r3} = \frac{\text{A[i]}}{\text{A[i + 3]}}, \quad (4)$$

$$\text{r4} = \frac{\text{A[i]}}{\text{A[i + 4]}}. \quad (5)$$

If the result is true, then the position of the marker center can be computed as (Eq. (6), Fig. 7a):

$$\begin{cases} X = \sum_{j=1}^{i-1} A[j] + \frac{1}{2} \sum_{j=i}^{i+4} A[j] \\ Y = \text{current row number} \end{cases}. \quad (6)$$

Then the program scans along the X- axis(Fig. 7b). The process is similar to that of the Y- axis scan, and the marker center is calculated by (Eq. (7)):

$$\begin{cases} X = \text{current of column number} \\ Y = \sum_{j=1}^{i-1} A[j] + \frac{1}{2} \sum_{j=i}^{i+4} A[j] \end{cases}. \quad (7)$$

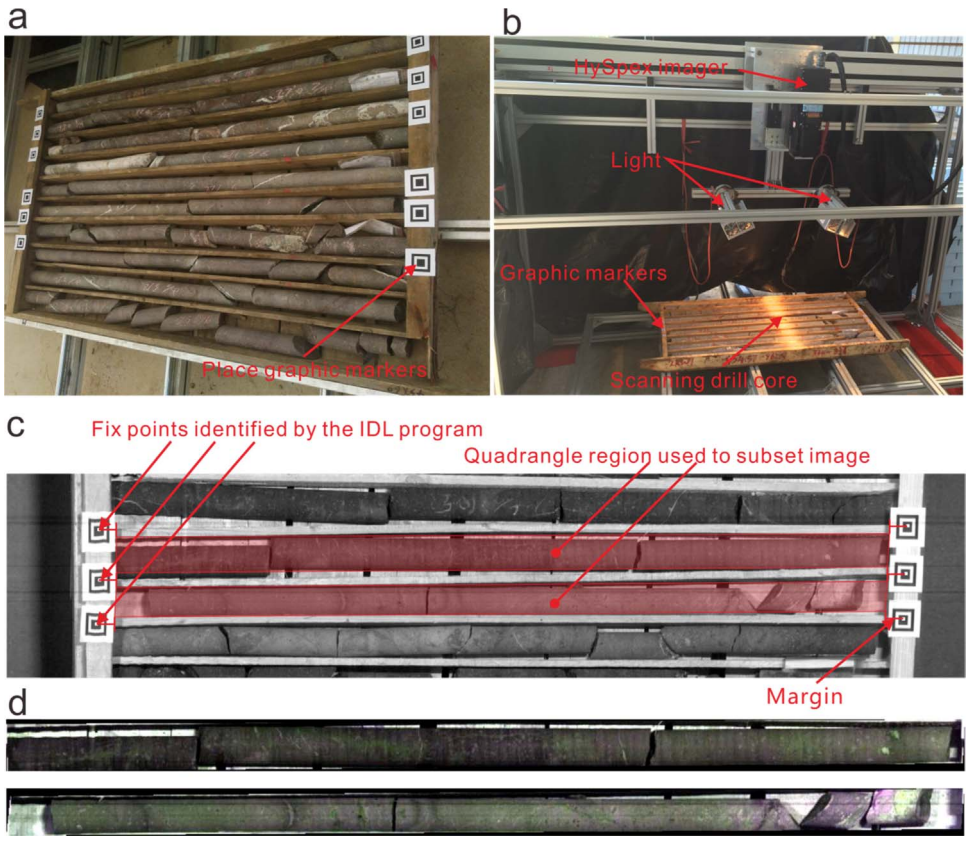

Fig. 3. (a) Graphic markers are placed at the ends of the core box. (b) Scanning of the cores and box by a hyperspectral imager. (c) The IDL program recognizes the locations of the graphic markers and creates quadrangles to subset the image. (d) The results of subset hyperspectral images.

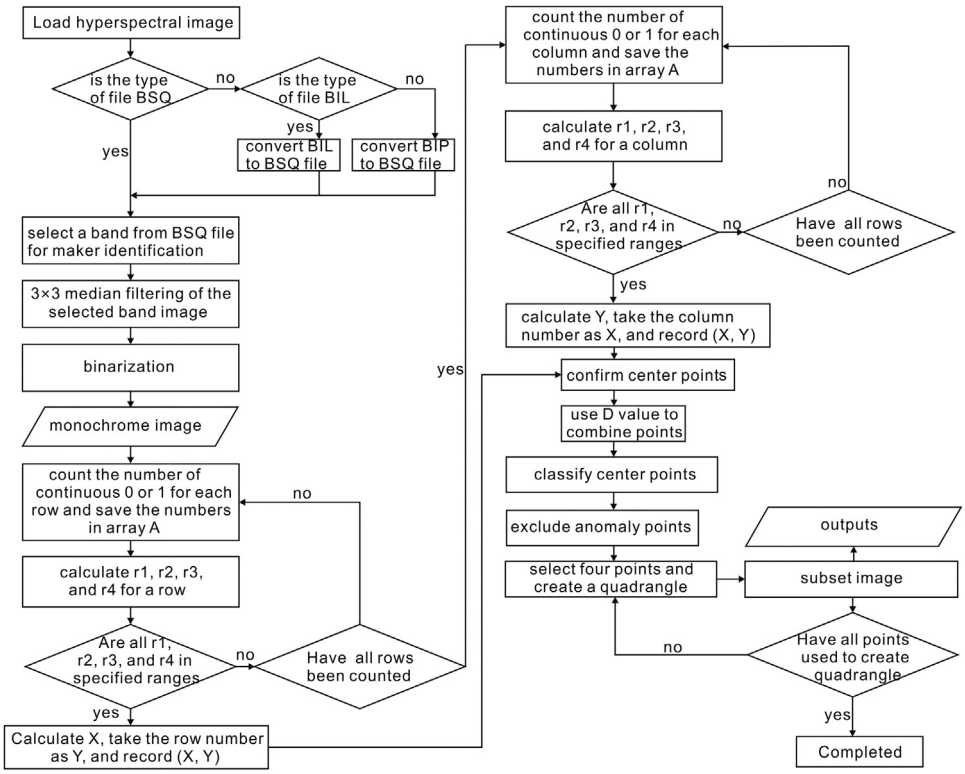

Fig. 4. Flow chart of the image processing procedure.

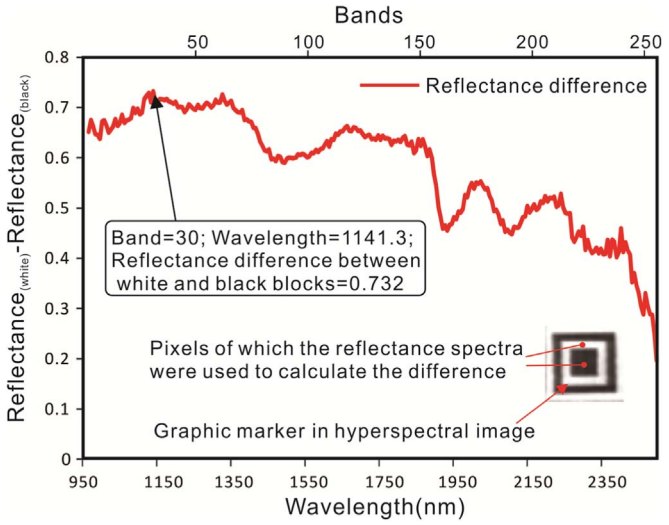

Fig. 5. Relationship between the reflectance difference of white and black blocks and wavelength. The reflectance difference is greatest (0.732) at 1141.3 nm (band 30).

The true center points are those that can be found in both the X- and Y- axis scans (Fig. 7).

The white blocks of the markers, which are more reflective than the threshold value, should be assigned as 1, while the darker black block should be 0. However, sources of related to the imager or environment (e.g., limitations of the spatial resolution of the imager, or mixed -pixels), may result in incorrect block assignments. This results in ratios of block widths that are slightly different from the nominal values (1:1:3:1:1); thus, no marker can effectively be identified unless a tolerance is used.

The IDL program introduces a tolerance value, developing the criteria for marker identification into:

$$r1 \in [1 - t,\ 1 + t],$$
$$r2 \in [0.3333(1 - t),\ 0.3333(1 + t)],$$
$$r3 \in [1 - t,\ 1 + t],$$
$$\text{and } r4 \in [1 - t,\ 1 + t],$$

where t is tolerance value.

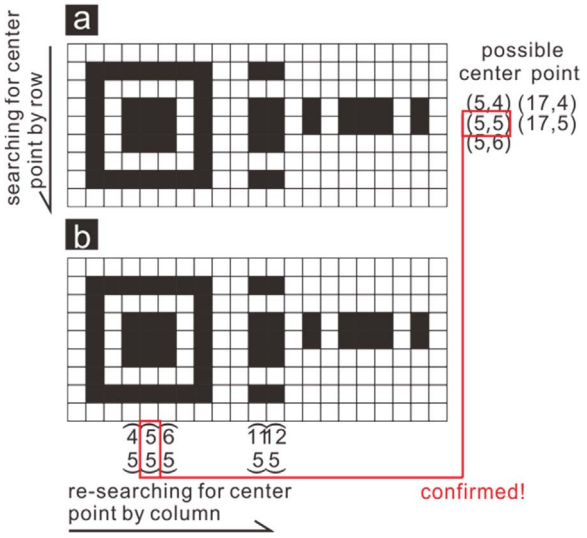

Fig. 7. (a) The program first searches for center points by row. (b) The center points are confirmed by re-searching the center points by column. True center points are those identified both in X and Y scans.

The use of tolerance value can lead to false identification: too narrow a tolerance value may lead to false negative results, while too large a tolerance value may cause false positives. In this study, we propose two methods for mitigating false negatives, and use outlier examination test to exclude false positives. There are two effective ways to avoid false negatives: (1) increase the marker size, and (2) increase the tolerance value. In (1), more space is required for each marker, which becomes problematic when the diameter of the drill core is small; whereas (2) may lead to an increase in the number of false positives.

To understand how marker size and tolerance values influence marker identification using the HySpex imager, we compared groups of markers of four different sizes (14 mm/19 pixels, 21 mm/28 pixels, 28 mm/37 pixels, and 35 mm/47 pixels). Markers were placed on cardboard (15 markers in each group) and scanned with the imager (Fig. 8a). The IDL program was then applied at different tolerance

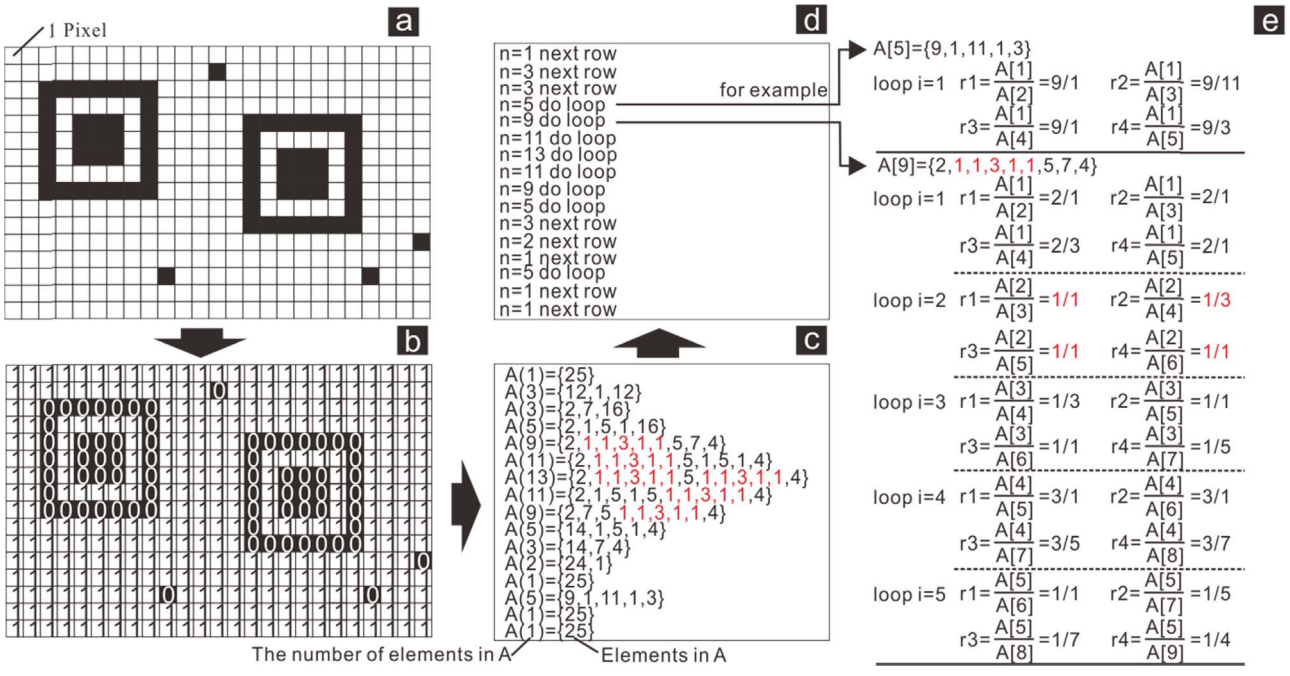

Fig. 6. Examples of two markers in (a) a band image, and (b) a monochrome image. (c) The numbers of continuous 0 or 1 elements are stored in array A. (d) A loop will be carried out if the number of elements in A is greater than five. (e) The program performs the loop and calculates r1, r2, r3, and r4.

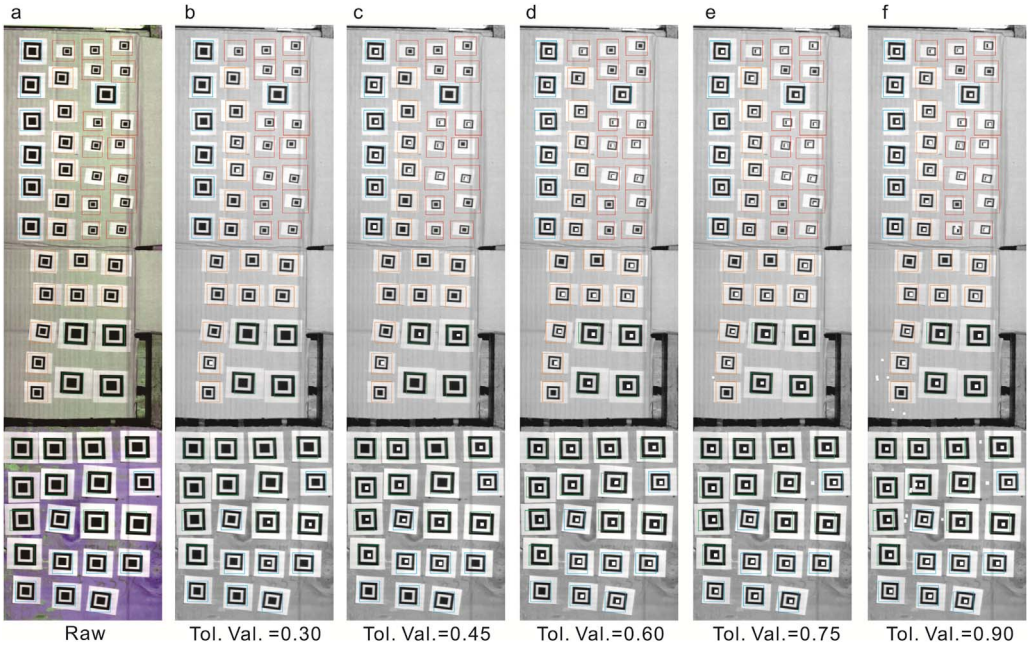

Fig. 8. (a) Examples of the different sizes of graphic markers used for marker size selection. (b–f) Results of marker recognition for different tolerance and marker sizes. The markers of the different groups are indicated by the colors of the rectangles: red for group 1 (marker size: 14 mm/19 pixels), orange for group 2 (marker size: 21 mm/28 pixels), blue for group 3 (marker size: 28 mm/37 pixels), and green for group 4 (marker size: 35 mm/47 pixels). (Tol. Val.= Tolerance value).

Table 2
False positives and negatives at different tolerance values and marker sizes.

Tolerance	False positive	False negative			
		14 mm/19 pixels	21 mm/28 pixels	28 mm/37 pixels	35 mm/47 pixels
		(group 1)	(group 2)	(group 3)	(group 4)
30%	0	15	12	14	13
45%	0	10	12	5	5
60%	0	7	3	1	0
75%	2	4	3	0	0
90%	14	3	3	0	0

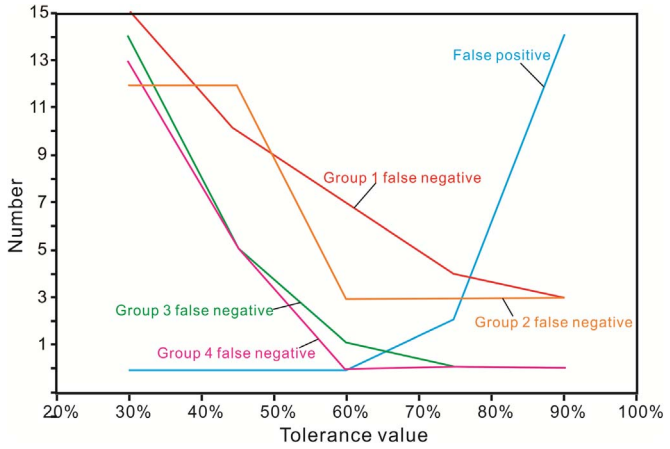

Fig. 9. False positives and negatives at different tolerance values and marker sizes. The marker sizes for group 1–4 are: 14 mm/19 pixels, 21 mm/28 pixels, 28 mm/37 pixels, and 35 mm/47 pixels, respectively.

values. The results are listed in Table 2 and shown in Figs. 8b, c, d, e, f, and 9.

The results show that the markers in the two smallest size groups were poorly recognized, even when the tolerance value was 90%. The two larger marker sets were well identified when the tolerance value was greater than 75%, and the largest set (35 mm/47 pixels) was completely recognize when the tolerance value was 60%, at which value no false positive was found. Interestingly, markers in the third group (28 mm/37 pixels) were all identified only when the tolerance was greater than 75%, at which value two false positives are discovered.

3.2.6. Identification of center points

The introduction of a tolerance (and thus a ratio range) for marker identification leads to the possibility of more than one center point being recognized by the program. A distance value, D, is therefore employed to address this issue (D can be customized by the user, and is set here to be equal to the pixel width of the marker). Fig. 10 shows that if the distance among n center points (X1,Y1; X2, Y2; ...; Xn, Yn) is less than D, they will be regarded as the same point, whose center position (X, Y) is calculated as (Eqs. 8 and 9, Fig. 10):

$$X = \frac{1}{n}\sum_{i=1}^{n} X_i, \tag{8}$$

$$Y = \frac{1}{n}\sum_{i=1}^{n} Y_i. \tag{9}$$

3.2.7. Classification of points

The software then classifies each center point as belonging to either the top or bottom group, based on the Y values. Points with Y values greater than the average Y value are classified into the bottom group; the others are classified into the top group (Fig. 11).

3.2.8. Exclusion of anomalous points

The top and bottom groups of the markers' center points might also contain false positives (Fig. 11). Each group of center points should

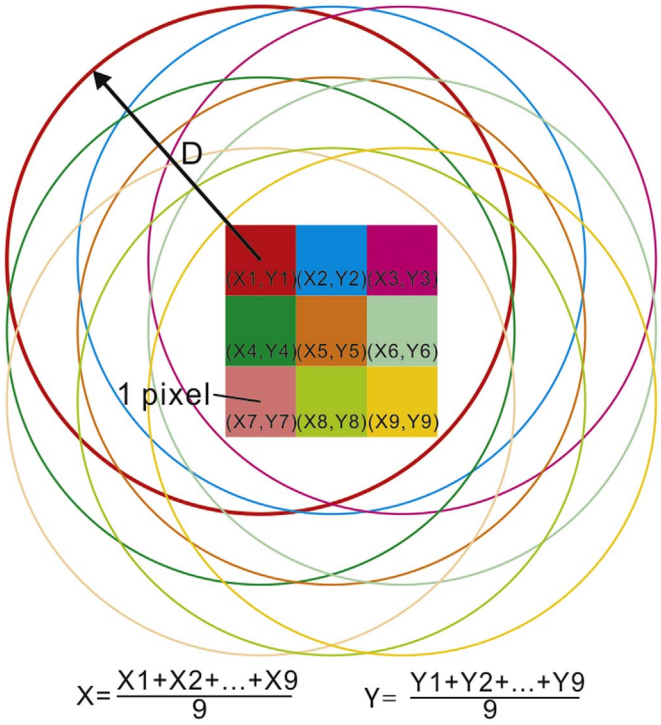

Fig. 10. The D value is used to combine nearby points. If the identified center points are separated by less than D, they will be combined as a single new point with a new center coordinate.

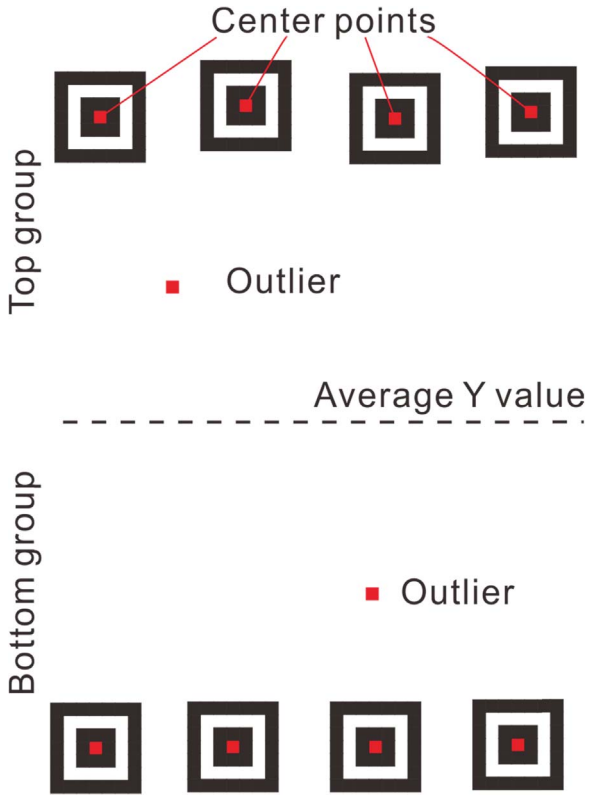

Fig. 11. The center points are classified into two groups according to their Y values, which should be similar within each group. False positives have Y values outlying from either group, and can be excluded using outlier examination test.

have similar Y values, while the false positives will have distinct Y values (i.e., they are outliers of their group). If the number of points in a group is equal to or larger than 3, the IDL program will perform outlier examination following the guidelines below:

The IDL program first finds the maximum and minimum Y values and computes the range (the difference between the maximum and minimum values) for a group. If the range is smaller than 200 (the value can be customized by users), the test will end and no outlier will be excluded; otherwise the IDL program creates two new arrays: one excluding the maximum value, and the other excluding the minimum value. The IDL program computes the new ranges for the two arrays, and sends the array with smaller range into the next-turn outlier examination.

3.2.9. Creation of the quadrangle and subsetting the image

The program repeatedly selects two neighboring points from the top group and two corresponding points from the bottom group to create a quadrangle (Fig. 12a). Its borders are represented by four straight-line equations (Fig. 12b) that form the boundary determining whether a pixel lies within the quadrangle (Fig. 12b). Pixels within the quadrangle will be stored, while those outside the quadrangle will be set to 0 and removed from the dataset.

4. Application and result

Based on the selection criteria developed in Sections 3.2.2 and 3.2.5, and considering that some drill cores are ~3.5 cm in diameter, we chose band #30 for marker identification, using 28 mm × 28 mm(37 pixels × 37 pixels) markers with a tolerance value of 75%.

We obtained hyperspectral imagery of the drill cores using the HySpex SWIR-320m-e system, and stored the images in an input folder named “in” (Fig. 13a). After creating an output folder named “out”, we ran the IDL program, and set the input and output folder paths (Fig. 13b). The IDL program automatically processed the hyperspectral images, and stored the results in the “out” folder (Fig. 13c).

Eighteen drill cores were subsetted by the IDL program. Visual inspection of the subset images confirms that all of the cores had been subsetted successfully, and none of the box remained. Appendix I overviews the input and output hyperspectral images. Fig. 14 shows monochrome (Fig. 14a) and marker identification images (Fig. 14b) of the third box of drill cores. A total of eight points were identified by the IDL program, including two outliers on the right side of the image (Fig. 14b). The two outliers are far from the three center points on the right edge of the core box. The outliers were successfully excluded by outlier examination test, and the subset core images are shown in Fig. 14c.

5. Discussion

Although the drill cores and core boxes have different colors due to variable mineral compositions and covering materials, we successfully performed automatic subsetting of hyperspectral imagery of drill cores using the proposed method, which suggests that the method was not affected by the color of the drill core, or by the color or type of material of the core box. Given that four identifiers were used to create a quadrangle region, a skewed core box would not significantly influence image subsetting. As each graphic marker is symmetrical and can be recognized at any angle, the drill core can be correctly subsetted even when the Y-axis of the core box is not strictly parallel to the scanning track of the imager. In addition, the space between pairs of markers can be customized to fit drill cores of different sizes. This method is accessible to virtually all researchers in the field because the markers used as identifiers are very cheap to produce, and no advanced computer processing is required.

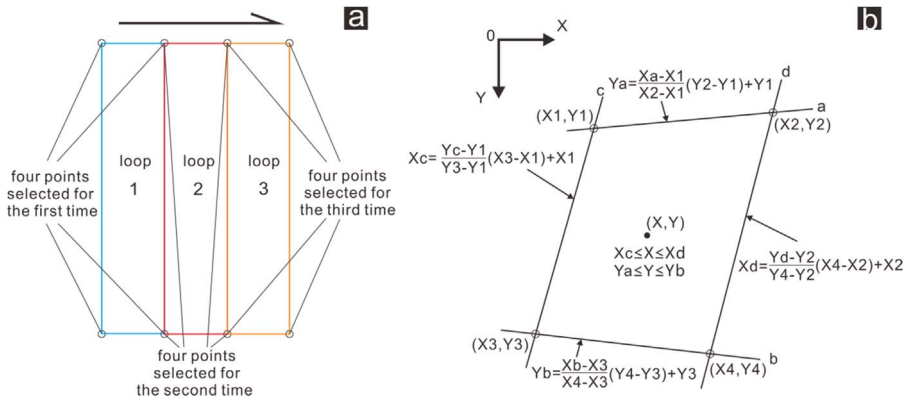

Fig. 12. (a) The program selects two neighboring points from the top group and the corresponding two points from the bottom group to create a quadrangle. (b) Four straight-line equations define the borders of the quadrangle, and are the basis for determining whether a given pixel is in it.

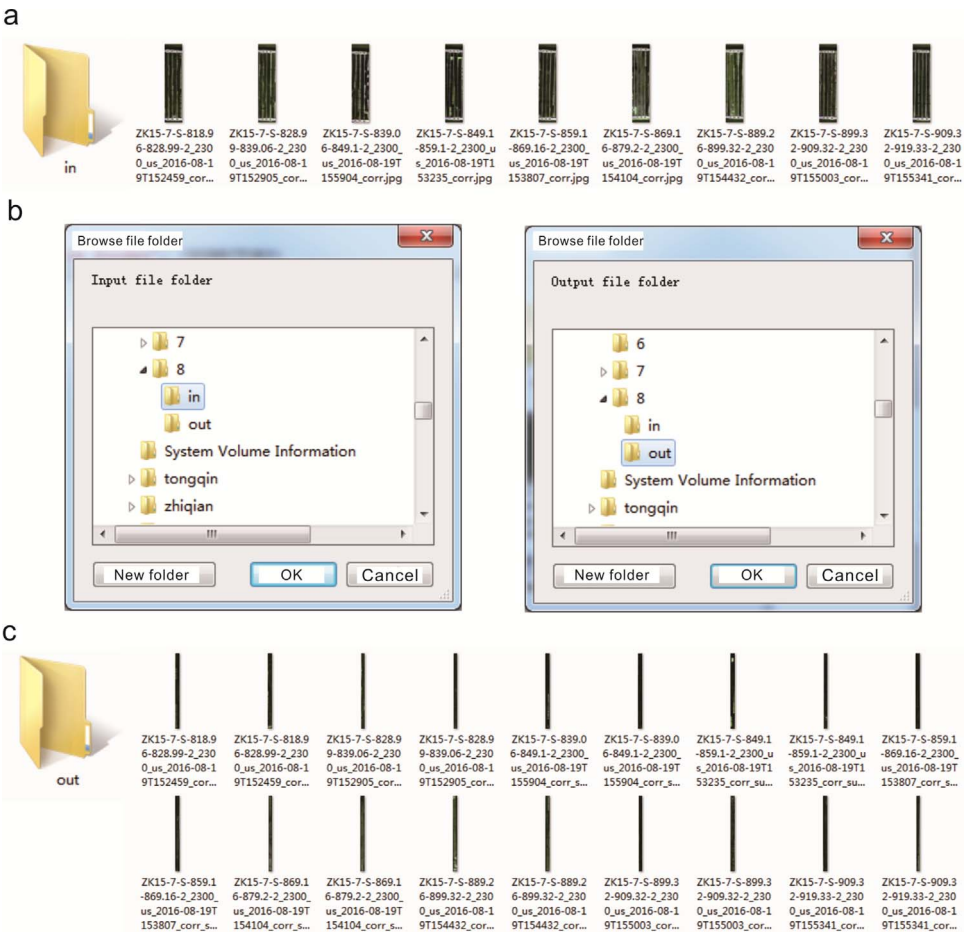

Fig. 13. (a) Hyperspectral images are placed in the input folder named "in". (b) The input and output folder paths are set. (c) The IDL program subsets the image, and stores the results in the output folder named "out".

6. Conclusions

(1) Our IDL program can subset hyperspectral imagery of drill core with high accuracy, and the subsetting process can be performed efficiently.
(2) Ideal values for ratio variation tolerance, minimum marker size, and suitable wavelength for marker identification using the HySpex SWIR-320m-e imager are: 75%, 37×37 pixels (28 mm × 28 mm), and 1141.3 nm (band 30), respectively.
(3) The proposed method is unaffected by deformation of the core box or by variation in the size of the drill core. Subsetting is achievable even if the Y-axis of the core box is not absolutely parallel to the scanning track of the imager.

Note

The IDL program can be download at Pangaea database (www.pangaea.de). Hyperspectral images are too large to be uploaded; please contact the author for the original hyperspectral images if required.

Fig. 14. Imaging of cores within a core box. (a) Monochrome image; (b) Marker identification image showing the center points identified by the program, including two false positives. (c) The resulting subset core image.

Acknowledgements

This study was financially supported by the National Natural Science Foundation of China (41601008 and 41502037) Longcan Project of China National Nuclear Corporation (LCD116-4), Concentrated Research Development Project of China National Nuclear Corporation (Comprehensive application study on hyperspectral remote sensing for uranium and multi-metal ore exploration, YLTY1604), the Youth Foundation of Beijing Research Institute of Uranium Geology (YQJ1601), and the GF-5 Project of China (04-Y20A35-9001-15/17)

Appendix A. Supporting information

Supplementary data associated with this article can be found in the online version at doi:10.1016/j.cageo.2017.05.009.

References

Baissa, R., Labbassi, K., Launeau, P., Gaudin, A., Ouajhain, B., 2011. Using HySpex SWIR-320m hyperspectral data for the identification and mapping of minerals in hand specimens of carbonate rocks from the Ankloute Formation (Agadir Basin, Western Morocco). J. Afr. Earth Sci. 61, 1–9.

Dorador, J., Rodriguez-Tovar, F.J., 2016. High resolution digital image treatment to color analysis on cores from IODP Expedition 339: approachimg lithologic features and bioturbational influence. Mar. Geol. 377, 127–135.

Kruse, F.A., 1996. Identification and mapping of minerals in drill core using hyperspectral image analysis of infrared reflectance spectra. Int. J. Remote Sens. 17, 1623–1632.

Kruse, F.A., Bedell, R.L., Taranik, J.V., Peppin, W.A., Weatherbee, O., Calvin, W.M., 2012. Mapping alteration minerals at prospect, outcrop and drill core scales using imaging spectrometry. Int. J. Remote Sens. 33, 1780–1798.

Mathieu, M., Roy, R., Launeau, P., Cathelineau, M., Quirt, D., 2017. Alteration mapping on drill cores using a HySpex SWIR-320m hyperspectral camera: application to the exploration of an unconformity-related uranium deposit (Saskatchewan, Canada). J. Geochem. Explor. 172, 71–88.

Murphy, R., Monteiro, S.T., 2013. Mapping the distribution of ferric iron minerals on a vertical mine face using derivative analysis of hyperspectral imagery (430–970 nm). ISPRS J. Photogramm. Remote Sens. 75, 29–39.

Qu, H., Zhang, F., Wang, Z., Yang, X., Liu, T., Ba, H., Wang, X, D., 2016. Quantitative fracture evaluation method based on core-image logging: a case study of cretaceous Bashijiqike formation in ks2 well area, Kuqa depression, Tarim Basin, NW China. Pet. Explor. Dev. 43, 465–473.

Speta, M., Gingras, M.K., Rivard, B., 2016. Shortwave infrared hyperspectral imaging: a novel method for enhancing the visibility of sedimentary and biogenic features in oil-saturated core. J. Sediment. Res. 86, 830–842.

Speta, M., Rivard, B., Feng, J., Lipsett, M., Gingras, M., 2015. Hyperspectral imaging for the determination of bitumen content ini Athabasca oil sands core samples. AAPG Bull. 99, 1245–1259.

Tappert, M.C., Rivard, B., Fulop, A., Rogge, D., Feng, J., Tappert, R., Stalder, R., 2015. Characterizing Kimberlite dilution by crustal rocks at the Snap Lake diamond mine (northwest territories, Canada) using SWIR (1.90–2.36 μm) and LWIR (8.1–11.1 μm) Hyperspectral imagery collected from drill core. Econ. Geol. 110, 1375–1387.